Studies of dust and gas in the interstellar medium of the Milky Way

Salgado Cambiazo, F.J.

Chapter 1

Introduction

1.1 The Interstellar Medium of the Milky Way

Most of the light we see with our eyes on a dark night is produced by stars. However, a fraction of approximately 10 to 15 % of the mass of the Milky Way is in the interstellar medium (ISM), i.e. material between the stars. Stars are born from the ashes of previous generations of stars in the dense molecular clouds of the ISM and, as stars evolve, stars also inject energy into the ISM in the form of radiation, winds and jets. At the end of their lives, stars release larges amount of material back into the ISM and massive stars also release copious amounts of kinetic energy in the form of supernovae explosions. The material released becomes the seed of new generations of stars. This interplay between stars and the interstellar medium shapes and drives the evolution of galaxies.

The interaction of stars and gas in galaxies leads to the formation of the different phases of the ISM and manifests itself as a rich and complex dynamical system. The phases of the ISM are generally described as composed by three main phases (McKee and Ostriker, 1977; Cox, 2005) together with transient (shorter lived) clouds. In Figure 1.1, we show a diagram describing the different phases of the ISM.

Massive stars (O and B stars) play an important role as they emit a large fraction of their luminosity at ultraviolet wavelengths. In particular, these stars emit at wavelengths shorter than the ionization potential of hydrogen and they ionize hydrogen in their surrounding volume producing HII regions. In the boundary between their natal molecular cloud and the ionized volume a photodissociation region (PDR) is formed. In this region non-ionizing stellar photons dissociate molecules and ionize atoms with low ionization potentials (e.g. C, S, Na) and heat the gas.

As most of the EUV photons created by massive stars are consumed by gas inside the HII regions, a large fraction of the ISM is in a neutral state. Actually, most of the neutral ISM is a PDR (Hollenbach and Tielens, 1999). This neutral gas is divided in two regimes that are often considered to be in pressure equilibrium (Savage and Sembach, 1996; Cox, 2005): the cold neutral medium (CNM), viz. discrete clouds with low filling factor ($\sim 1\%$), low temperatures (~ 100 K) and densities ~ 50 cm^{-3}; and the warm neutral medium

(WNM) with temperatures of $\sim 10^4$ K and densities of ~ 0.1 cm^{-3} with a larger filling factor ($\sim 30\%$). These neutral phases are embedded into a warm and a hot ionized gas with filling factors of 20% to 70%. The warm ionized gas corresponds to regions where hydrogen ionizing photons escape from HII regions, and the hot ionized medium corresponds to old supernova remnants (McKee and Ostriker, 1977; Spitzer, 1990; Wolfire et al., 2003). Due to gravity, material is clumped together into molecular clouds, the densest regions of the Galactic ISM, where new stars are formed. A summary of representative temperatures and densities of the phases of the ISM is given in Table 1.1 (adapted from Ferrière 2001).

In the CNM, hydrogen is neutral, but stellar photons with energies between 11.2 and 13.6 eV can ionize carbon atoms. The diffuse clouds that compose the CNM are heated by photoelectric effect on PAH and dust grains. The cooling of the gas is dominated by emission of the [CII] at 157 μm far-infrared structure line. There is a large resemblance between the CNM and PDRs, in other words, the CNM can be described as a low density PDR. The lifecycle of the ISM plays an important role in th evolution of galaxies as the repository of the nucleosynthetic products from stars and the birth of new generation of stars. This cycling of material is not well understood, largely because of the lack of suitable observational probes. The radiative interaction of stars with their environments in the dense PDR of region of massive star formation (HII regions and PDRs) requires sensitive observations at mid and far infrared wavelengths which contain key diagnostic lines. This wavelength region has only opened with the launch of Spitzer in 2003 and Herschel in 2009. SOFIA is continuing this IR revolution.

The CNM and WNM are generally studied using transition lines at UV and optical wavelengths and observations of the 21 cm hyperfine transition of neutral atomic hydrogen (e.g. Weaver and Williams 1973; Kalberla et al. 2005; Heiles and Troland 2003b). However, deriving physical properties from UV and optical lines is difficult, as these tracers are affected by dust extinction. Deriving physical parameters of the neutral structures of the ISM from the 21 cm line is challenging because separating the cold and warm components is difficult (e.g. Heiles and Troland 2003a). In this work, we explore the of the IR emission to probe HII regions and PDRs and of low frequency carbon radio recombination lines to study the properties of gas in the CNM as a first step to towards understanding the lifecycle of the ISM in the evolution of galaxies.

1.2 Low Frequency Carbon Radio Recombination Lines

The ionization potential of carbon is lower than that of hydrogen and carbon can be ionized in regions where hydrogen is largely neutral such as the CNM.

Table 1.1: Main characteristics of the phases of the ISM (Ferrière, 2001).

ISM Phase	T (K)	n (cm^{-3})	Hydrogen state
Molecular	10-20	100-10^6	Molecular
Cold neutral	50-100	20-50	Neutral atomic
Warm neutral	6000-10000	0.2-0.5	Neutral atomic
Warm ionized	8000	0.2-0.5	Ionized atomic
Hot ionized	10^6	~ 0.0065	Ionized atomic

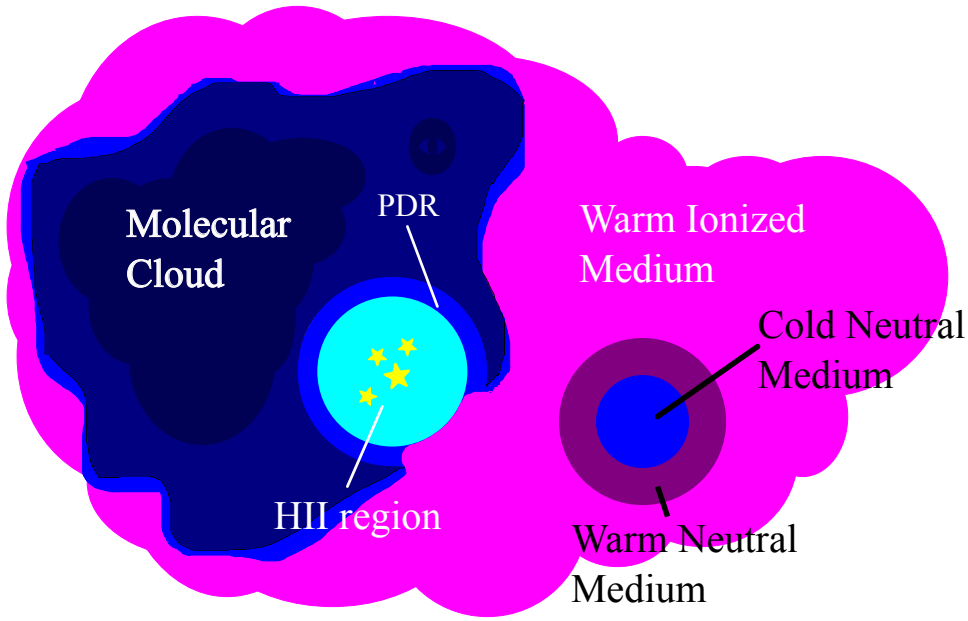

Figure 1.1: A schematic representation of a region in the interstellar medium of the Milky Way.

Lines produced by carbon can be used as probes of the physical properties of the ISM. In particular, transitions between high Rydberg states leads to the production of Carbon Radio Recombination Lines in the sub-millimeter to decameter range. At these long wavelengths, dust extinction is not important, in contrast to UV and optical carbon lines.

1.2.1 CRRL Observations

The first carbon recombination lines in the radio regime (5 GHz) were detected in emission towards NGC 2024 and IC 1795 (Palmer et al., 1967). Nowadays, these "high" frequency carbon recombination lines are known to be occur in PDRs associated with HII regions and have been detected towards other known HII regions (e.g.: Balick et al. 1974; Knapp et al. 1976a; Pankonin et al. 1977; Vallee 1987, 1989; Roelfsema and Goss 1991; Natta et al. 1994; Garay et al. 1998; Quireza et al. 2006) and reflection nebula (e.g.: Brown and Knapp 1974; Knapp et al. 1976b; Pankonin and Walmsley 1978b,a). Crutcher (1977) detected carbon recombination lines in emission towards ζ Ophiuchi and *o* Persei. In contrast to the lines detected by Palmer et al. (1967), the lines detected by Crutcher (1977) are associated with cold diffuse clouds.

The first low frequency (26.1 MHz) CRRL was detected in absorption towards the supernova remnant Cas A by Konovalenko and Sodin (1980) and it was wrongly attributed to a hyperfine structure line of ^{14}N (Konovalenko and Sodin, 1981). This first detection corresponds to a transition occurring between high quantum levels ($n = 631$). After this first detection, several other low and high frequency CRRLs have been observed towards Cas A (e.g. Ershov et al. 1984; Anantharamaiah 1985; Sorochenko and Walmsley 1991; Anantharamaiah et al. 1994). Recently, transitions involving levels as high as $n = 1009$ have been observed (Stepkin et al., 2007). This transitions correspond to the largest atoms found in space, with sizes of about 50 μm. Erickson et al. (1995) performed a survey of the Galactic plane (from Galactic longitude $l = 340^\circ$ to $l = 20^\circ$) at 76 MHz using the 64 m telescope at Parkes Observatory. With a large beam of 4° they detected lines in roughly 50 fields. Kantharia and Anantharamaiah (2001) presented observations at 34.5 MHz using the low-frequency dipole array (at Gauribidanur, India) with an angular resolution of $\sim 21' \times 25\,\mathrm{deg}$; and at 327 MHz using the Ooty Radio Telescope with two angular resolutions ($2^\circ \times 2^\circ$ and $2^\circ \times 6'$). Nine out of the 32 regions observed at 34.5 MHz were detected in absorption, while seven out of the twelve were detected in emission at 327 MHz with seven detections being common to both frequencies. Roshi et al. (2002) expanded the Galactic survey in search for recombination lines at 327 MHz using the Ooty Radio Telescope. As Kantharia and Anantharamaiah (2001) they used two angular resolutions ($2^\circ \times 2^\circ$ and $2^\circ \times 6'$) and concluded that diffuse C^+ regions show structure from $6'$ to 5° and structure over $\sim 6'$ owing to clumps.

The above mentioned studies show that CRRLs are widespread throughout the Galaxy; however, observations of low frequency CRRLs has been challenging because CRRLs are intrinsically faint with line to continuum ratios of about 10^{-4} to 10^{-3}. Even for the CRRLs detected towards Cas A, arguably the strongest CRRLs observed up to this date, the observed optical depth of

the line is $\sim 10^{-3}$. Furthermore, detailed interpretation of the results has been hampered by the velocity resolution of the instruments used to observe the lines, e.g. the line widths observed by Kantharia and Anantharamaiah (2001) are dominated by Galactic rotation. Therefore, to study low frequency CRRLs from the ISM, sensitive observations at high angular and velocity resolution are required.

1.2.2 LOw Frequency ARray (LOFAR)

The Low Frequency Array (LOFAR, van Haarlem et al. 2013) is an aperture synthesis array composed of phased array stations. The antennas in each station form a phased array, producing one or many station beams on the sky. Multi-beaming is a major advantage of the phased array concept. It is not only used to increase observational efficiency, but may be vital for calibration purposes. The phased array stations are combined into an aperture synthesis array. The Remote Stations are distributed over a large area in the Netherlands and Europe. There are two distinct antenna types: the Low Band Antenna (LBA) operates between 10 and 90 MHz and the High Band Antenna (HBA) between 110 and 250 MHz. The stations are distributed over an area about one hundred kilometers in diameter (located in the North-East of the Netherlands). Other stations are located in Germany, Sweden, the UK and France.

LOFAR is opening the low frequency sky to systematic studies of low frequencies carbon radio recombination lines due to its increased sensitivity and high angular resolution. Recent high angular resolution (beam size of $40''$) observations of CRRLs using LOFAR towards the line of sight of Cas A (Asgekar et al., 2013) have shown the structure of the clouds towards the supernova remnant. Moreover, the high spectral resolution of LOFAR allow us, for the first time, to separate the multiple velocity components towards Cas A (Oonk et al., 2015a; Salas, 2015) even at low frequencies. Furthermore, new detections towards Cyg A (Oonk et al., 2014) and the first extragalactic detection in the starburst galaxy M82 (Morabito et al., 2014a) demonstrate the high potential of LOFAR for CRRLs investigations.

Pilot studies have demonstrated that surveys of low frequency radio recombination lines of the galactic plane are within reach, providing a new and powerful probe of the diffuse ISM. These new observations have motivated us to reassess the recombination line theory, relax some of the approximations made by previous works and to expand the range of applicability of in terms of temperature, density and the importance of external radiation fields on the strength of the lines.

1.2.3 Carbon Radio Recombination Line models

The use of CRRLs as probes of the ISM requires detailed modeling to interpret the observations. After the first observations of carbon recombination lines at high frequencies(Palmer et al., 1967), it was proposed by Goldberg and Dupree (1967) that the observed properties were not compatible with local thermodynamic equilibrium. Instead, they determined that the level population was enhanced by dielectronic recombination. Zuckerman and Palmer (1968) suggested that the "anoumalous microwave recombination line" was due to carbon in the outer parts of HII regions. Later observations confirmed that the high frequency carbon recombination lines originated in HI regions surrounding the ionized gas of the HII region (i.e. a PDR). Studies of low temperature carbon lines towards PDRs were carried out by (Brocklehurst, 1973), Dupree (1974) and Hoang-Binh and Walmsley (1974).

The discovery of low frequency CRRLs observations by Konovalenko and Sodin (1981) demonstrated the presence of Rydberg Carbon atoms in space. These observations challenged the theory of carbon recombination lines and new models were required to interpret the observations. Later theoretical works by Watson et al. (1980); Walmsley and Watson (1982a) showed that, at low temperatures ($T_e \lesssim 100$ K), electrons can recombine into carbon ions by simultaneously exciting the ${}^2P_{1/2} - {}^2P_{3/2}$ fine structure line. Watson et al. (1980); Walmsley and Watson (1982a) modified the model from Brocklehurst (1970) for hydrogen recombination lines to include the dielectronic recombination process. There are two important assumptions in Brocklehurst (1970) model: the assumption of an statistical distribution of the angular momentum levels, and an asymptotic behavior of the level population towards local thermodynamic equilibrium. The first assumption is not valid if dielectronic processes need to be included. Therefore, in order to incorporate the dielectronic process into the model, a prescription is given by Walmsley and Watson (1982a) that takes into account the non-statistical distribution of angular momentum levels by considering the angular momentum changing collisions.

The dielectronic recombination process occurs to high n states and can explain the behavior of the high n CRRLs observed towards Cas A (Walmsley and Watson, 1982b). Ponomarev and Sorochenko (1992) suggested to compute the level population of the ${}^2P_{1/2} - {}^2P_{3/2}$ fine structure line self consistently. A new class of models was proposed by Payne et al. (1994), where the assumption of the level population tending to equilibrium at high quantum level was replaced by a complete depopulation of these high-n states.

Incorporating information from the [CII] line can provide additional information on the physical properties of the observed clouds, theoretical work in this direction was carried out by Natta et al. (1994); Sorochenko and Tsivilev (2000).

It is of importance to mention that all these previous theoretical works tried to explain the observations towards Cas A. In particular, the integrated optical depth as a function of quantum number. As we mention in the previous section, these observations were carried out with single dish telescopes with large beams and low velocity resolution and at high quantum number the quality of the observations is poor (see e.g. Payne et al. 1994).

However, new observations carried out by LOFAR have been able to separate the multiple components (see Figure 1.2). This new LOFAR observations have motivated the studies of CRRLs presented here. In this work we make use of increased computer power to solve the level population problem considering a much large number of levels than ever before. Furthermore, recent works (Vrinceanu et al., 2012) have updated the collisional rates values, providing more accurate results on the level population distribution and, consequently, to better models for the lines. In Figure 1.3, we exemplify this by showing a fit to the LOFAR Cas A data Oonk et al. (2015a). In Figure 1.4, we show how restrictions from CRRLs observations together with the [CII] at 158 μm can be effectively used to constraints the density and temperature of the intervening clouds.

1.3 HII Regions and Photodissociation Regions

Massive stars are formed in dense molecular clouds, the exact process to form massive stars is currently not well understood and two main mechanisms have been proposed: monolithic collapse and competitive accretion (e.g. McKee and Ostriker 2007; Zinnecker and Yorke 2007). Regardless of the mechanism, as a massive star turns on it releases a large amount of ultraviolet energy at wavelengths shorter than the ionization potential of hydrogen (13.6 eV, EUV photons) creating a bubble of ionized gas known as a HII region. The increase in temperature and pressure in the HII region leads to an expansion of the ionized volume, at this stages the HII region is referred to as ultra compact and compact. The expansion continues until the bubble bursts out and the gas inside the ionized bubble vents out into the ISM, reaching the state of a champagne flow (Tenorio-Tagle, 1979; Wood and Churchwell, 1989; Churchwell, 2002). We summarize the properties of HII regions at different evolutionary stages in Table 1.2 adapted from (Kurtz, 2005).

The expansion of the HII region leads to the creation of a photodissociation region (PDR), where far-ultraviolet (FUV) stellar photons can penetrate into the molecular cloud and dissociate molecular hydrogen. In addition, photons with energies larger than 11.2 eV can ionize carbon atoms. Due to high density and dust extinction, photons with longer wavelengths are absorbed deeper in the PDR leading to an "onion-like" ionization/molecular structure (Tielens and

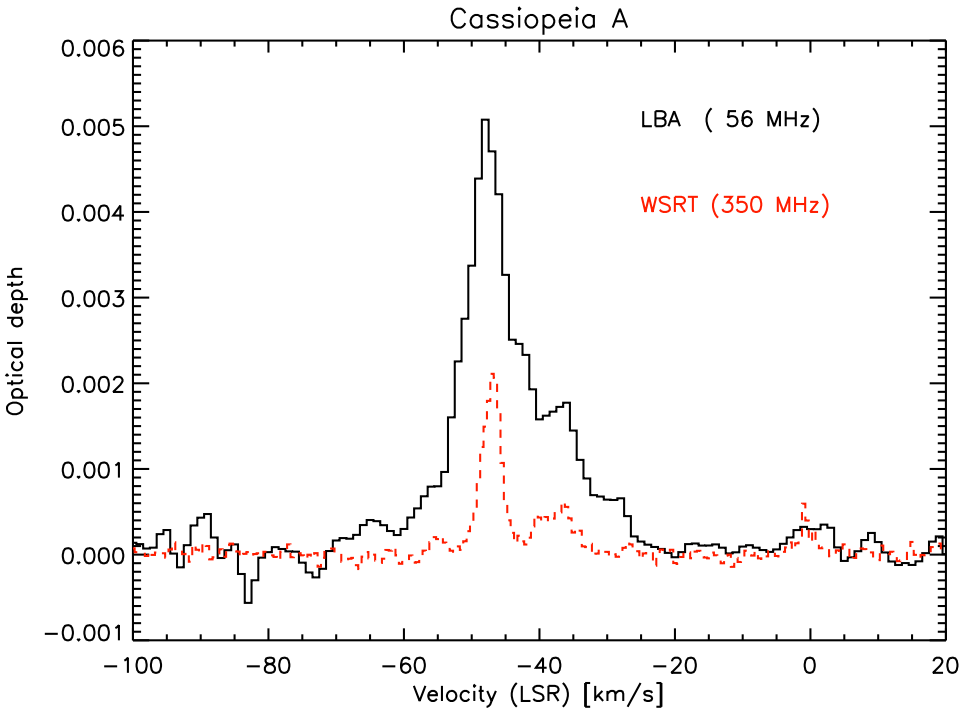

Figure 1.2: A comparison of LOFAR LBA spectra at 56 MHz and WSRT observations at 350 MHz, the high velocity resolution of LOFAR allow us to separate the cloud components even at low frequencies where line broadening from radiation dominates (Oonk et al., 2015a).

Hollenbach 1985; Hollenbach and Tielens 1999, Figure 1.5). In the inner regions of the PDR, H_2 and CO remain in their molecular form as the stellar photons reaching these zones are not energetic enough to dissociate these molecules.

The heating of PDRs is mainly produced by photoelectric effect (e.g. Bakes and Tielens 1994), viz. photons with wavelengths in the FUV regime ionize small grains and PAHs and the electrons ejected out of the grains heat the surrounding gas. The temperature of the gas is determined by the balance between the photoelectric heating and gas cooling. Cooling is dominated by emission of far-infrared fine structure lines [CII] at 157 μm and [OI] at 63 μm, with minor contribution to the cooling due to CO and H_2 emission.

Early studies using the IRAS satellite (Neugebauer et al., 1984) showed that at infrared wavelengths HII regions are strong emitters. This emission is produced by dust grains heated by radiation emitted by the central star. However, due to the low spatial resolution of IRAS ($\sim 4'$), mostly global energetic assessments could be done. More recent studies using higher resolution instru-

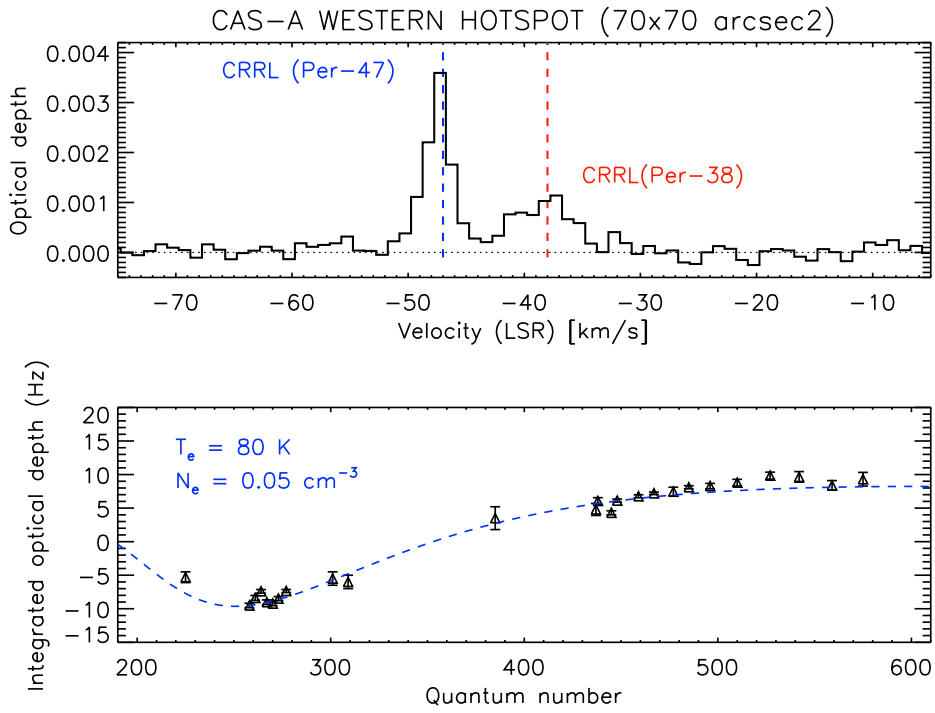

Figure 1.3: Upper panel: An spectra of the Cas A (Salas, 2015) at 355 MHz two components can be clearly seen at −47 and −38 km s^{-1}. Lower panel: a fit to a combined data set from the literature (Payne et al., 1989; Kantharia et al., 1998), WSRT, LOFAR observations of the CRRLs in the −47 km s^{-1} component towards Cas A.

ments with ISO (Peeters et al., 2002) and *Spitzer* (GLIMPSE and MIPSGAL survey, Benjamin et al. 2003; Churchwell et al. 2009; Carey et al. 2009) have greatly expanded our knowledge on the spatial distribution of dust in HII regions. Deharveng et al. (2010) showed that extended bright emission at 24 μm is spatially associated to ionized gas, as traced by 20 cm continuum emission. On the other hand, 8 μm emission is associated with the PDRs surrounding the ionized gas.

1.4 PAH and Dust Grains

Dust grains are an important component of the ISM. Mostly composed by two distinct chemically different species: carbonaceous and silicates, dust grains contribute to reddening and extinction at ultraviolet and optical wavelengths, absorbing stellar light and re-emitting it at longer wavelengths, thus dominat-

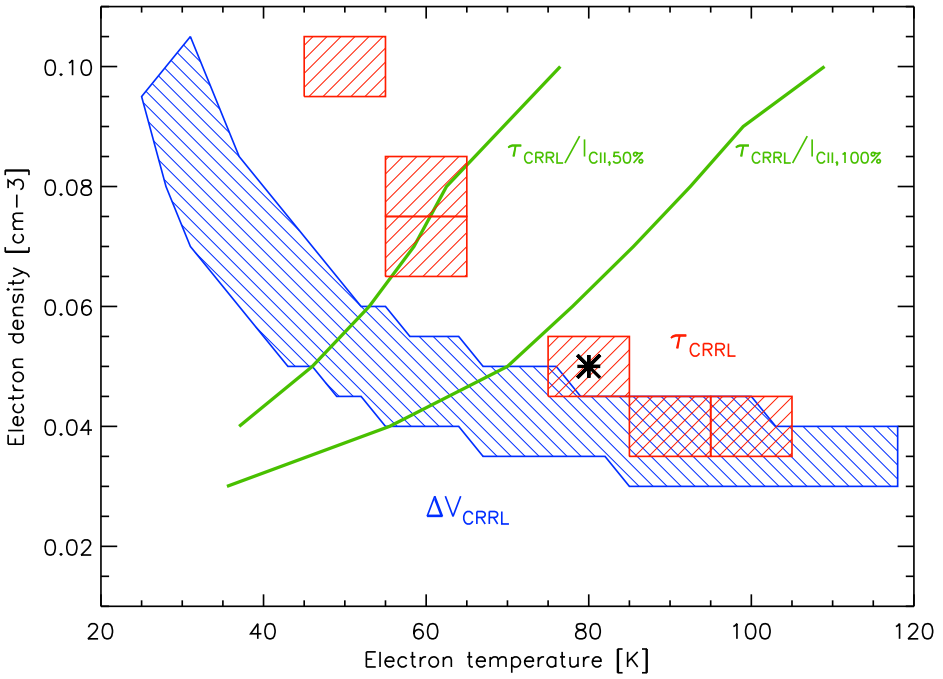

Figure 1.4: An example of the use of CRRLs together with [CII] line (green lines) and line width constraints (blue regions) towards Cas A (Oonk et al., 2015a). The star marks the model with the best fit, red boxes show other good fits to the data. The physical properties of the cloud can be well constrained.

Table 1.2: Physical characteristics of HII regions (Kurtz, 2005).

ISM Phase	n (cm^{-3})	size (pc)
Hyper Compact HII region	$\gtrsim 10^6$	0.03
Ultra Compact HII region	$\gtrsim 10^4$	~ 0.1
Compact HII region	$\sim 10^3$	~ 0.5
Classical HII regions	$\sim 10^2$	~ 10

ing the emission at infrared to sub-millimeter wavelengths. The luminosity of (ultra) luminous infrared galaxies [(U)LIRGs] and starburst galaxies is largely emitted through dust emission. Dust infrared emission can be a convenient tracer of star formation rate (e.g. Calzetti et al. 2007). Infrared emission due to dust in galaxies has been detected at redshifts as high as $z \approx 9$ (e.g. Watson et al. 2015) and is an important probe of the properties of galaxies at high

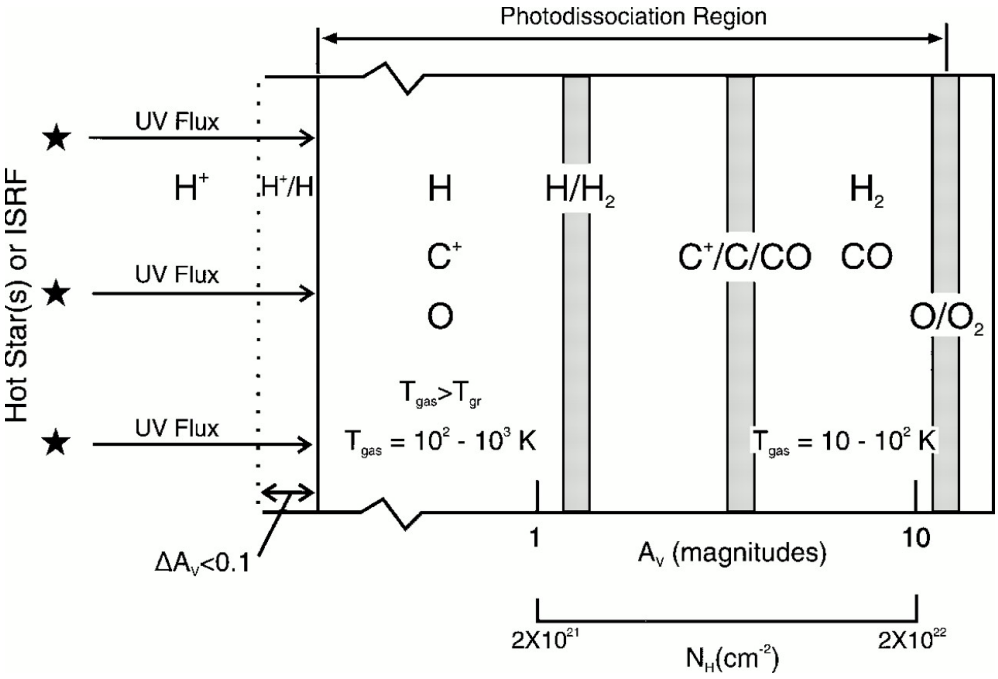

Figure 1.5: A schematic representation of a photodissociation region.

redshifts. At low temperature and large densities, molecules can form on the surface of dust grains driving the chemistry of the ISM. Moreover, in protoplanetary discs, dust grains are the building blocks of rocky planets such as Earth (e.g. Blum and Wurm 2008; Krijt et al. 2015).

Dust grains show a distribution in size ranging from small polycyclic aromatic hydrocarbons (PAH, large carbonaceous molecules formed by carbon rings) to micron size carbonaceous and silicate grains (Draine, 2003; Zubko et al., 2004). Extinction measurements show that the dust size distribution changes within the Galaxy (e.g. Cardelli et al. 1989). It has been shown that the size distribution of dust grains can be described by a power law $n(a) \propto a^{-3.5}$, with a the radius of a grain. This power law is usually referred to as the MRN distribution from Mathis et al. (1977) (e.g. Draine 2003). It is generally accepted that dust grains are formed by condensation in the wind of asymptotic giant branch (AGB) stars, Wolf-Rayet stars, novae and in the ejecta of supernovae (e.g. Draine 2009). However, the actual injection rates are very uncertain and it is usually believed that a large fraction of dust is produced in the ISM.

As dust grains interact with gas and radiation, the properties of dust change

and these changes are related to the environment. Therefore, it is important to understand how dust properties change. During their time in molecular clouds dust grains can grow through accretion of ice mantles and coagulation (Ossenkopf and Henning, 1994; Ormel et al., 2011). In contrast, dust grains can be easily destroyed in shocks by sputtering, releasing their constituent material back to gas phase. Other sources of dust destruction include vaporization when grains are exposed to strong radiation fields and shattering due to grain-grain collisions (Tielens et al., 1994; Jones et al., 1996).

In Figure 1.6, we show models for dust emission in two environments: the diffuse ISM and a dense PDRs. It can be seen that the light emitted by dust grains is mostly observed at wavelengths between 1 and 1000 μm. However, observations at these wavelengths are difficult from earth because the atmosphere of Earth blocks a large fraction of the light (upper panel in Figure 1.7).

1.5 SOFIA FORCAST

The Stratospheric Observatory for Infrared Astronomy (SOFIA) consists of a telescope of 2.7 m in diameter aboard a modified Boeing 747SP. By flying at high altitudes (12 to 14 km), it can observe above the water vapor layer of the atmosphere where the infrared atmospheric transmission is greatly increased (Figure 1.7). SOFIA started its observations in May 2010 and is planned to have a lifetime of 20 years. Details about SOFIA early observations and capabilities can be found in Young et al. (2012).

Among the first instruments on SOFIA is the Faint Object InfraRed Camera for the SOFIA Telescope (FORCAST, Herter et al. 2012). FORCAST is a two channel mid-infrared camera with a short wavelength detector (SWC) ranging from 5 to 25 μm and a long wavelength detector (LWC) covering from 25 to 40 μm. Images can be obtained using the detectors individually or simultaneously, by using a dichroic mirror. In addition, FORCAST also is capable of grism spectroscopy in the 5-50 μm range. The wavelength coverage of FORCAST is perfectly suited for studying dust emission in HII regions and PDRs as the peak of the dust SED is expected to be located at these wavelengths (cf. Figure 1.6). In addition, the relatively large field of view of the FORCAST camera ($\sim 3.2' \times 3.2'$) and the pixels scale ($0.768''$/pixel) makes the instrument well suited to observe extended regions in the Galaxy. Now that SOFIA is in operations, detailed spatially resolved (see Table 1.3) studies of dust emission from HII regions have come in reach. The studies of HII regions presented in this thesis are among the first that have made use of these new capabilities offered by SOFIA to characterize dusty HII regions.

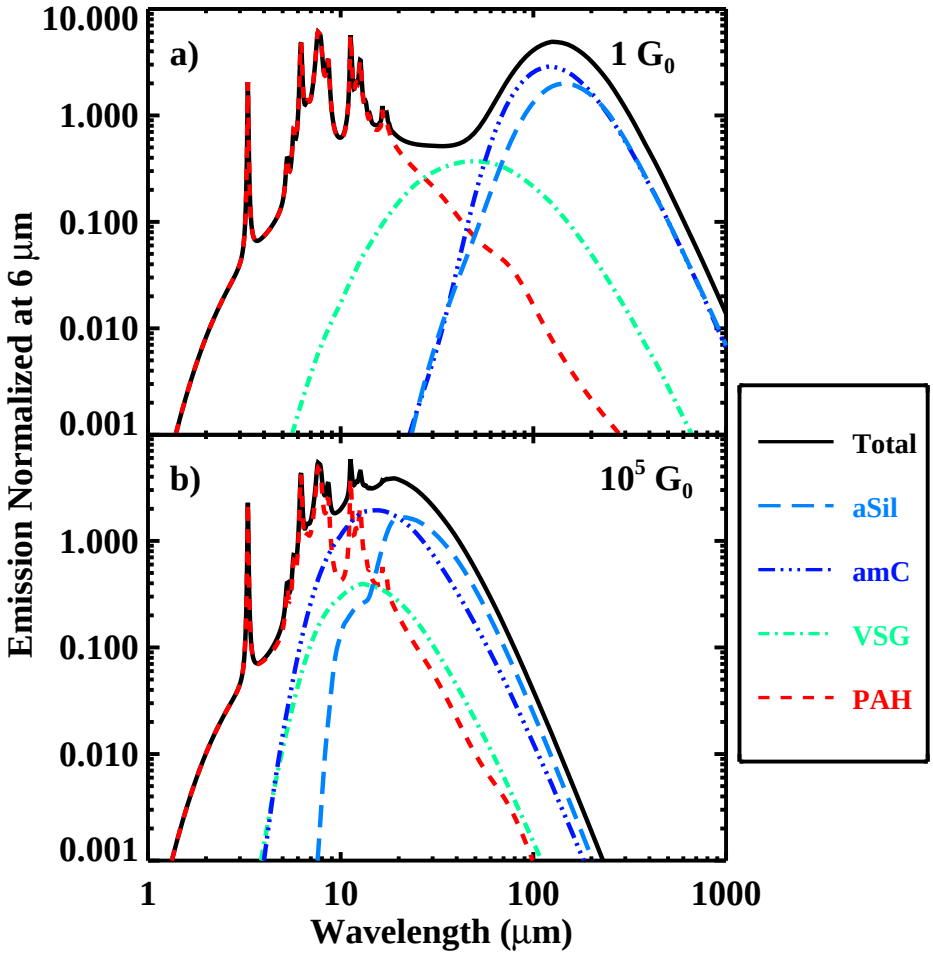

Figure 1.6: Dust emission produced by the Dustem code (Compiègne et al., 2011) in two cases: a) Under the FUV local radiation field (1 G_0 = 1.6 × 10^{-3} erg s^{-1} cm^{-2}), similar to the radiation field observed by the diffuse ISM. b) Under a radiation field larger than the local FUV radiation field (10^5 G_0), similar to the radiation field observed by a PDR close to a massive star. Red lines correspond to emission produced by PAHs, cyan lines by very small grains, light blue is emission produced by large carbonaceous grains and dark blue by silicates.

1.6 This Thesis

This Thesis can be considered to have two parts: in the first one we present a study of the dust properties in HII regions and their surrounding PDRs. We

Table 1.3: Filters characteristics and resolution of FORCAST for the filters used in this work.

Wavelength (μm)	$\Delta\lambda$ (μm)	FWHM ($''$)
6.4	0.14	2.9
6.6	0.24	3.0
7.7	0.47	2.7
19.7	5.5	2.9
31.5	5.7	3.4
37.1	3.3	3.6

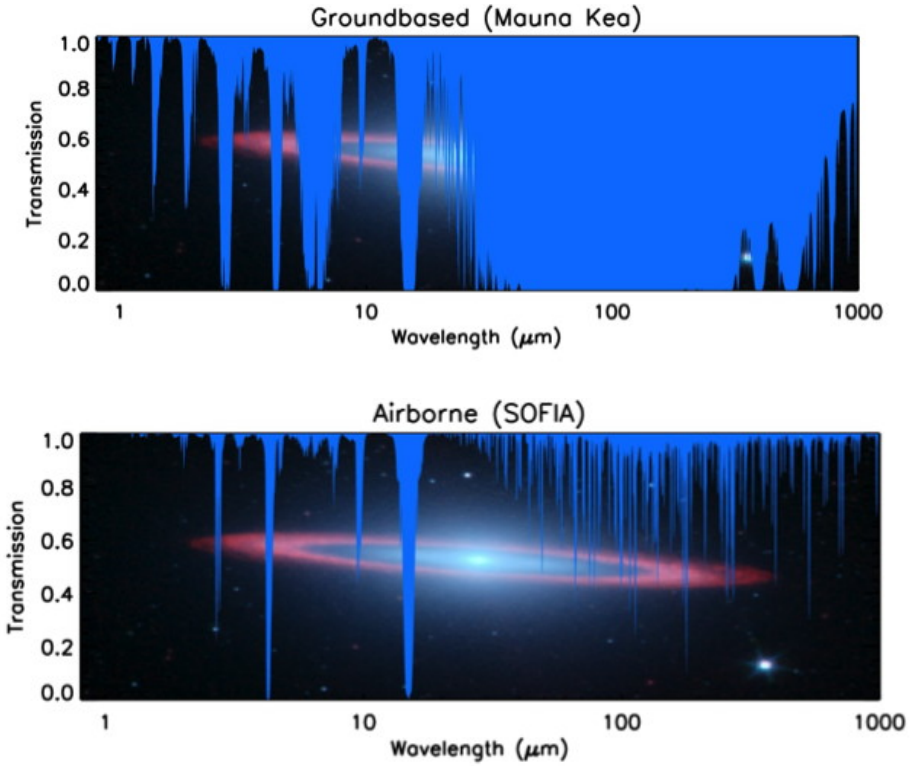

Figure 1.7: Comparison between the atmospheric transmission at Mauna Kea and that achieved by SOFIA. The atmospheric transmission is greatly increased at wavelengths larger than 20 μm at the altitudes that SOFIA is able to observe.

focus our studies on two compact HII regions: W3(A) and the Orion Nebula. The second part of this thesis presents theoretical studies of the properties of the cold neutral medium using carbon radio recombination lines.

In Chapter 2, the study towards W3(A) is presented. We used SOFIA/FORCAST photometry to characterize the dust emission in the region. The photometry is used to construct spectral energy distribution (SED) maps to study the dust abundance and temperature in this region. A strong spatial correlation between dust emission and ionized gas tracers is found. By using the properties of the star, a simple model is proposed with dust and gas well mixed within the ionized gas. The dust in the ionized gas must have different properties as compared to dust in the diffuse ISM in order to explain the size of the region.

A study of dust grains in the Orion Nebula is presented in Chapter 3. The Orion Nebula is one of the best studied star forming regions and a wealth of supporting data is available at all wavelengths. In this work, we show new observations performed by SOFIA with the FORCAST instrument. The SOFIA/FORCAST data is complemented with *Herschel*/PACS photometry. This allow us to characterize the complete infrared SED of the region including the far infrared tail of dust emission. We compare the FORCAST and PACS images with data from the literature and find that the PACS images trace a cold dust component located in the molecular cloud. The FORCAST data is found to be produced by warm dust in the HII region and by the background PDR. We characterize the dust properties in the PDR and the HII region and, as for W3(A), the dust properties must be different to those in the diffuse ISM. A comparison of dust emission and cooling lines is used to characterize the photoelectric heating efficiency in the Orion Bar PDR.

In Chapter 4, we construct models to determine the level population of atoms at low temperatures and densities. The focus of this study is to characterize the level population of carbon atoms under the (non-LTE) conditions of the diffuse ISM in terms of departure coefficients. Based on hydrogenic models from the literature, we expand the range of validity of approximations to the high quantum levels of the observed radio recombination line transitions. Among the physical properties that determine the level population, the most critical parameter to accurately model for the level population is the dielectronic recombination.

In Chapter 5, we used the level population models from Chapter 4 to model the line emission and absorption towards clouds with temperatures and densities of the CNM. We analyze the line widths properties and solve the radiative transfer equation assuming a model for the galactic synchrotron radiation field and the cosmic microwave background (CMB) emission. The models are used to describe methods for how to use CRRL observations to determine the physical properties more effectively and we provide illustrative examples using data from the literature. These models are currently being used to determine the physical conditions of diffuse atomic clouds observed with LOFAR.

1.7 Future Outlook

In coming years, new telescopes are expected to start operating. These new instruments will further increase our knowledge on the physics of the ISM and the studies presented in this thesis will be expanded.

As the Planck results (Planck Collaboration et al., 2011) as well as the observations presented in this thesis demonstrate, properties of dust in regions of massive star formation are very different from those of dust in the diffuse ISM. The launch of the James Webb Space Telescope (JWST) is expected to occur in October 2018 and will greatly expand this field. With a telescope of 6.5 m, JWST will carry the largest mirror ever launched into space. Among the instruments onboard JWST, the Mid-Infrared Instrument (MIRI) will be able to perform imaging and spectroscopical studies of dust in HII regions from 5 to 28 μm with high angular resolution and high sensitivity. The spectroscopic and photometric capabilities of JWST/MIRI can extend the study of HII regions in our galaxy to much fainter levels as well as to nearby galaxies and thus probe a much larger range of physical characteristics (density, metallicity, stellar cluster size, etc.) at unprecedented resolution. Such studies will be key to understand observations of massive star formation at redshifts of ~ 1.

As the first LOFAR studies demonstrate and the results of this thesis quantify, CRRLs provide a powerful probe of the physical conditions in the cold phases of the ISM. The Square Kilometer Array (SKA) will be the next generation of low frequency observatories and will greatly improve our studies on CRRLs. Being located in the southern hemisphere, SKA will be able to map the Galactic Center and the Magellanic Clouds in search for CRRLs. SKA will be perfectly suitable for Galactic studies of the large scale behavior of CRRLs as well as small scale (pinholes) and extragalactic studies (Morabito et al., 2014a).